Food & Function

Accepted Manuscript

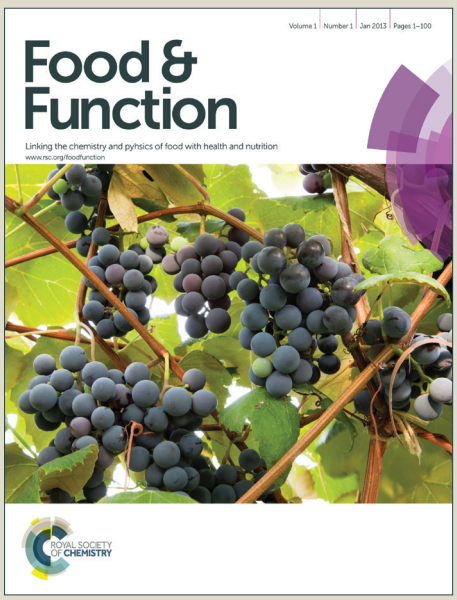

This is an *Accepted Manuscript*, which has been through the Royal Society of Chemistry peer review process and has been accepted for publication.

Accepted Manuscripts are published online shortly after acceptance, before technical editing, formatting and proof reading. Using this free service, authors can make their results available to the community, in citable form, before we publish the edited article. We will replace this *Accepted Manuscript* with the edited and formatted *Advance Article* as soon as it is available.

You can find more information about *Accepted Manuscripts* in the Information for Authors.

Please note that technical editing may introduce minor changes to the text and/or graphics, which may alter content. The journal's standard Terms & Conditions and the Ethical guidelines still apply. In no event shall the Royal Society of Chemistry be held responsible for any errors or omissions in this *Accepted Manuscript* or any consequences arising from the use of any information it contains.

ROYAL SOCIETY OF CHEMISTRY

www.rsc.org/foodfunction

OIL BINDING CAPACITIES OF TRIACYLGLYCEROL CRYSTALLINE NANOPLATELETS: NANOSCALE MODELS OF TRISTEARIN SOLIDS IN LIQUID TRIOLEIN

M. Shajahan G. Razul[1], Colin J. MacDougall[1], Charles B. Hanna[2], Alejandro G. Marangoni[3], Fernanda Peyronel[3], Erzsebet Papp-Szabo[4] and David A. Pink*[1,3]

[1] Physics Department, St.Francis Xavier University, Antigonish, NS, Canada

[2] Department of Physics, Boise State University, Boise, ID, USA

[3] Guelph-Waterloo Center for Graduate Work in Physics, Department of Food Science, University of Guelph, Guelph, ON, Canada

[4] Department of Physics, University of Guelph, Guelph, ON, Canada

Abstract

Polycrystalline particles composed of triacylglycerol (TAG) molecules, and their networks, in anhydrous TAG oils find extensive use as edible oils in the food industry. Although modelling studies of TAG systems, have been carried out, none have attempted to address a problem of central concern to food science and technology: the "Oil binding capacity" of a system of such edible oils. Crystalline nanoparticles (CNPs) have recently been identified as the fundamental components of solid fats in oils. Oil binding capacity is an important concept regarding the ability of fats particles to retain oil, and the ability of these CNPs to bind oil is important in designing healthy foods. We have carried out atomic scale molecular dynamics computer simulations to understand the behavior of a triacylglycerol oil (triolein) in nanoscale confinements between tristearin CNPs. We define a nanoscale oil binding capacity function by utilizing the average oil number density, $<\Phi(d)>$, between two CNPs as a function of their separation, *d*. We modelled pure tristearin CNPs as well as tristearin CNPs in which the surfaces are covered with an interface comprising soft permanent coatings. Their surfaces are "hard" and "soft" respectively. We found that for a pair of hard-surface tristearin CNPs a distance *d* apart, (i) triolein exhibits number density, and therefore density, oscillations as a function of *d*, and (ii) the average number density between two such CNPs decreases as *d* decreases, viz. the oil binding capacity is lowered. When a soft layer of oil covers the CNP surfaces, we found that the oscillations are smeared out and that the average number density between the two CNPs remained approximately constant as *d* decreased indicating a high oil binding capacity. Our results might have identified important nanoscale aspects to aid in healthy food design.

Introduction

Polycrystalline particles composed of triacylglycerol (TAG) molecules, and their networks, in anhydrous TAG oils find extensive use as edible oils in the food industry. Although some studies of model TAG systems[1-3] have been carried out, none have attempted to address a problem of central concern to food science and technology: what are the factors which determine the "oil binding capacity" of a TAG crystalline network, viz. the ability of a crystallineTAG networks to retain liquid TAG oils. *Trans* and saturated fats play essential roles in the creation of such networks but such fats, particularly the industrially generated ones, are well known for their negative effects on health[4,5]. This has been recognized by the World Health Organization, and most medical associations around the globe, and great pressure is being exerted on the food manufacturing industry to reduce both *trans* and saturated fat used in food products, as well as increase the levels of "healthy" polyunsaturated fatty acids naturally present in liquid oils. Recently, the U.S. Food and Drug Administration proposed that the use of partially-hydrogenated oils should be denied GRAS status[6]. High-melting point, crystalline *trans* and saturated TAGs constitute the structuring solid material, from which the networks are formed, in edible fats. However, a reduction in the amount of these solid structuring materials leads to an increase in the proportion of free liquid TAG oil present in manufactured food products, with concomitant losses in food quality and stability. This loss in quality has defeated attempts to improve the nutritional quality of commonly consumed food products. Accordingly, it is important to understand what are the factors determining the oil binding capacity of fat crystal networks in order to know just what it is that has to be mimicked in order to replace the *trans* fats presently in use.

In recent years, seemingly fundamental components making up solid fats structures in edible oils have been identified as highly-anisoptropic crystalline nanoplatelets (CNPs), composed of layers of crystalline TAGs, with average dimensions of approximately 500 nm × 200 nm × 50 nm[7-10]. If these CNPs are indeed the fundamental components from which all larger scale fats structures are constructed, then it is important to understand how they interact with the surrounding oils and with each other.

In order to understand the physics of oil binding capacity we have modelled the thermodynamics and physical structures of liquid oil between a pair of solid surfaces. Specifically, we have modelled triolein oil in a confined nanoscale space between two tristearin surfaces. The intent is to attempt to shed light on whether, apart from the possible higher cost of creating single-component systems, those edible oils that find use in modern food technology must contain a mix of solid fats and complex many-component fluids in order to possess a high oil binding capacity. Can we present any evidence that a single-component oil can possess as high an oil binding capacity as does a many-component (fluid) oil? Is the characteristic of possessing many components essential for exhibiting a (sufficiently) high oil binding capacity? Edible oils which find a use can be described as "functional" - that is, they exhibit suitability for some culinary purpose.

Recently, we modelled the effect of having a soft interface between a single "hard" tristearin surface and triolein oil[11]. There it was shown that a two-component liquid oil formed from triolein and monooleic-dielaidic molecules would undergo separation on the nanoscale at the surface of the tristearin CNP so that the monooleic-dielaidic component was preferentially adsorbed onto the CNP surface.

This result suggested that we should model a CNP coated with an impenetrable soft coating in order to compare the oil binding capacity of uncoated tristearin CNPs in contact with triolein, with that of a coated tristearin CNP in contact with triolein.

Simple and complex fluids under confinement, including fluids confined between two walls (i.e., a "slit pore") have been studied theoretically and [11-23]and, in particular much work has been done on n-alkanes[24-28]. Typically, particles have been modeled as spheres that interact via Lennard-Jones 6-12 potentials, and the confining walls are treated as continua that produce a confining potential for the fluid that is essentially an integrated Lennard-Jones potential. Those simulations and calculations exhibited oscillations of the fluid density at sufficiently small wall separations due to the packing effects of fluid particles or polymers near walls.

In this work, we focus on calculations of the TAG oil density and the free energy between the walls of a slit pore composed of (solid) TAG fats and filled with (fluid) TAG oil. We assume that the solid TAG walls are essentially insoluble in the oil at the temperature of the simulation. We propose the hypothesis that complexity of the liquid TAG oil leading to preferential adsorption of some of its components onto the solid TAG surfaces is of importance in creating a high oil binding capacity and that a system with a single component oil will exhibit a low oil binding capacity. To achieve this we shall have to define what we mean by "oil binding capacity".

Apart from the theoretical work referred go above, this paper is not the place to review all work done on modelling or measuring forces on fluids between surfaces because very little of it is relevant to our system. Indeed, we are unaware of any work having been done on the confinement of liquid TAG molecules on a nanoscale between a pair of walls or in a slit pore composed of (hydrophobic) TAG crystalline solids. In particular, we know of no other modelling work that studies such a system in order to define and quantify oil binding capacity. The most closely-related experimental work has been done on anhydrous triolein between (hydrophilic) mica surfaces using a surface force apparatus [29,30]. Claesson et al[31] and Dedinaite et al[32] found that triolein molecules were likely oriented at the mica surface due to the triolein molecules adopting a trident conformation in accord with the charge distribution of the mica. However, Dedinaite et al[33] and Dedinaite and Campbell[34] studied mica surfaces coated with phospholipids via self-assembly. This changed the surface

from hydrophilic to hydrophobic resulting in triolein exhibiting no order at the surface. We shall compare the latter observations to our results.

Here we present results obtained using atomic scale molecular dynamics to compute the densities of a TAG, triolein, oil phase bounded by a pair of solid tristearin CNPs a distance *d* apart. Such a system satisfies our requirement that the solid CNPs are essentially insoluble in the oil phase. We shall represent the solid CNPs as continua with parallel faces so that analytical calculations can be performed. The liquid oil, however, will be represented by model molecules using atomic scale molecular dynamics. The justification for this is that the modes of molecular motion of the solids have a higher energy than those of the liquid oil. We shall model solids with two kinds of surfaces: one in which the surface is pure tristearin, which we denote as "hard", and one in which the tristearin surface is coated with a layer of liquid oil with a density between that of tristearin and triolein. Such a surface we call "soft". We envisage the second case arising as shown elsewhere[11]. This paper is focussed on how oil binding capacity might depend upon whether the surfaces of the crystalline nanoplatelets are hard or soft as described here. Such layers are most likely to come from the presence of minority components in the liquid oil. It would not be plausible to try to extend our nanoscale results to a macroscale without considering what larger scale structures arise. What this paper provides is a start into how to treat oil binding in macroscale structures from a knowledge of the nanoscale characteristics. We shall show that our model system with a hard surface in contact with a single component oil possesses a low oil binding capacity and then investigate whether the oil-binding capacity is increased if the CNPs possess soft surface coatings.

Model System

Figure 1 shows typical molecular constituents of the solids and the oil (A), a TEM image of the CNPs [6-9], the total model system (C), and our model of the interface of two triacylglycerol CNPs (1 and 3) as two parallel surfaces of CNPs separated by an intervening triacylglycerol oil (2) (D). The CNPs possess flat surfaces, which are parallel to each other and define the $x-y$ plane. The CNPs occupy the half-spaces $-\infty < x, y < \infty$ and $0 \le z < \infty$ (medium 1) and $-\infty < z \le -d$ (medium 3). Here we shall initially model two tristearin CNPs separated by a layer of triolein oil. In order to model this system, we must understand the energies involved.

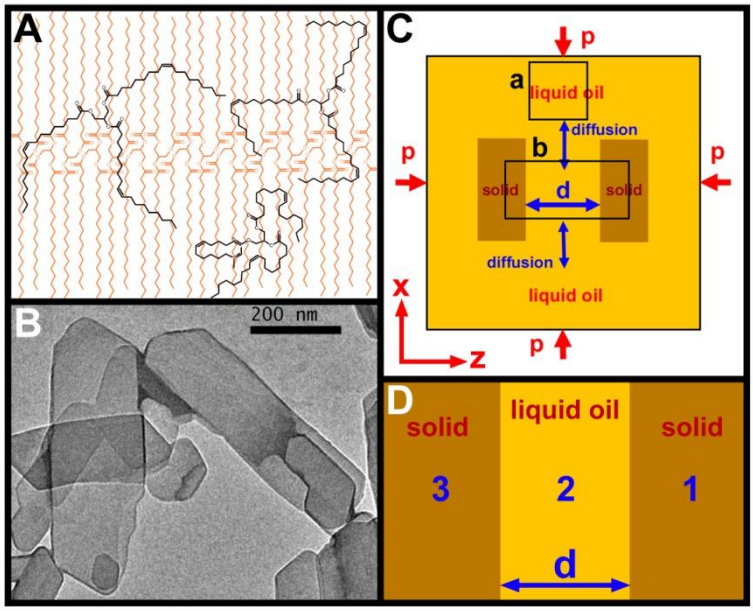

Figure 1. **A:** Diagram of triolein (foreground, black), showing the *cis* double bonds at carbon-9 of each acyl chain, and tristearin (background, brown) in a crystal. **B:** TEM image of Fully Hydrogenated Canola Oil (FHCO) nanocrystals. **C:** Schematic diagram of the simulation in the NpT ensemble showing a sample of the bulk (a) and the system of oil between two triacylglycerol CNPs (b). **D:** Schematic diagram of the system of parallel flat solid surfaces with oil between. Periodic boundary conditions apply along the $x-$ and $y-$axes.

Hard and Soft Interfaces

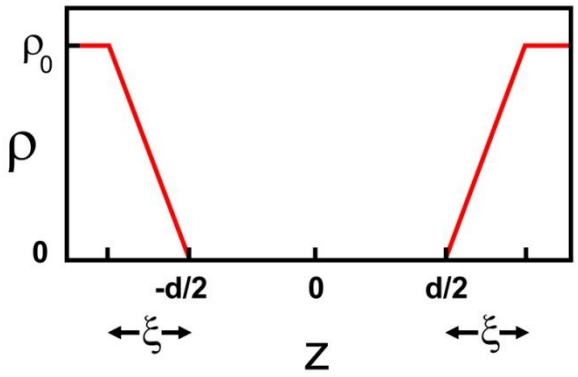

Figure 2. Model system densities. Two solids with constant density, ρ_0, filling two half spaces $-\infty < z < -\xi - d/2$ and $\xi + d/2 < z < \infty$. The two solids possess "soft" interfaces lying in the regions $-\xi -$

$d/2 < z < -d/2$ and $d/2 < z < \xi + d/2$ where the density changes linearly between 0 and ρ_0. In the limit as $\xi \to 0$ the solids possess "hard" interfaces for which the density exhibits a discontinuous change between 0 and ρ_0.

Figure 2 shows two realizations of Figure 1D. The more general case is that in which a solid fat with density ρ_0 has associated with it an interface possessing an average density that decreases to zero linearly with distance from the solid face. Such an interface could be liquid oils that have spontaneously phase separated from the majority triolein oil and become adsorbed onto the solid fat surface. We assume that this interfacial region is permanent. The region possesses a thickness ξ and we shall be considering two cases: (i) $\xi = 0$ so that the interface is "hard" and (ii) $\xi > 0$, a "soft" interface that interacts more weakly with triolein molecules than does the hard surface.

Interaction energies and the Hamaker coefficient

The Lennard-Jones (L-J) 6-12 potential, $u_{AB}(r)$, describing the van der Waals interaction between two spherically-symmetric atomic moieties, *A* and *B*, a centre-to-centre distance r apart is[29,30],

$$u_{AB}(r) = -\frac{C_6^{AB}}{r^6} + \frac{C_{12}^{AB}}{r^{12}} \quad (1)$$

If we assume that the solids and the oil are continua, that the oil density is constant, that the oil is distributed uniformly between the CNPs, and that density fluctuations can be ignored, then, using Mean Field theories, the dependence of the dispersion energy upon the CNP separation, *d*, is found to be proportional to $1/d^2$. This is obtained, in the usual way[29], by using cylindrical coordinates with the symmetry axis perpendicular to the surfaces (Figure 2) and integrating over all angles and one of the thicknesses of the half spaces. The Hamaker coefficient, A_{H123}, describing the interaction per unit area of surface, between media 1 and 3, each occupying the half-spaces of Figure 2, separated by medium 2, is defined as[29,30,35],

$$U_{123}(d) = -\frac{A_{H123}}{12\pi d^2} \quad (2)$$

Since we wish to study the structural characteristics of the liquid oil, such an approach is inadequate. The entire system is too complex to obtain closed analytical forms for measurable quantities; accordingly, we will model this system and carry out computer simulations. In order to not introduce unnecessary simplifications (*e.g.*, coarse grained models), we shall use atomic scale molecular dynamics.

Methods

Computer simulation. Atomic scale molecular dynamics (AMD). Here we report on AMD simulations performed using *NVT* ensembles with periodic boundary conditions employing the force field given by Berger, Edholm and Jähnig[36] and using the *V*-rescaled thermostat[37]. We used equation (1) and represented the solids and their interfaces as continua, but modelled the liquid as a molecular fluid using AMD. We modelled the radial interactions between 'non-bonded' triacylglycerol (TAG) atomic moieties using GROMACS[38,39]. TAGs possess only CH, CH_2, CH_3, O, and C=O moieties, and Tables are available which list the coefficients C_6^{AB} and C_{12}^{AB} that define the L-J potential between given pairs of these atomic moieties.

Strictly speaking, we should model a single system of two polycrystalline particles immersed in a bulk triolein fluid in the *NpT* ensemble, as shown in Figure 1C, with the molecules permitted to explore all of accessible space. This scenario is not practicable and, instead, we represented the bulk (Figure 1C (a)) and the system of Figure 1D (Figure 1C (b)) separately, and required that the chemical potentials of the two systems, calculated from the Helmholtz free energies, be equal. Our measured density of a bulk HOSO fluid (below) was used in the *NVT* ensemble for the bulk system of Figure 1C (a) with periodic boundary conditions. For the system of Fig.1D, the exploration of all possible tristearin CNP structures (single or multicrystals in one of α, β, β' phases, or combinations thereof) was not relevant to our intent. Instead, we represented the solids as continua with our measured density for crystalline FHCO (below). The interface, assumed to be composed of phase separated oils sufficiently tightly bound to the solid surfaces, was also represented as a continuum[40]. Accordingly, the averaged coefficients describing the interactions between an infinitesimal volume of a solid CNP and an atomic moiety labelled *B* in the triolein liquid were

$$\left\langle C_m^{\,B} \right\rangle = \sum_A n_A C_m^{\,AB} \qquad m = 6, 12 \qquad (3)$$

where n_A is the fraction of *A* atomic moieties of a tristearin in the CNP. This enabled us to represent the interaction energy, $U_{1B3}(d,\xi,z)$, between a pair of fat crystals possessing soft interfaces and an atomic moiety, B, of the triolein oil, possessing a *z*-coordinate z $(0<z<d)$ as

$$U_{1B3}(d,\xi,z) = V^1_{1B3}(d,\xi,z) + V^2_{1B3}(d,\xi,z) + V^3_{1B3}(d,\xi,z) \quad (4)$$

$$V^1_{1B3}(d,\xi,z) = 2\pi\Phi_1\mathcal{A}\left\{\frac{-\langle C_6^B\rangle}{12}\left[\frac{1}{(d/2+\xi-z)^3}+\frac{1}{(d/2+\xi+z)^3}\right]+\frac{\langle C_{12}^B\rangle}{90}\left[\frac{1}{(d/2+\xi-z)^9}+\frac{1}{(d/2+\xi+z)^9}\right]\right\} \quad (5)$$

$$V^2_{1B3}(d,\xi,z) = -2\pi\Phi_1\mathcal{A}\frac{d/2}{\xi}\left\{\frac{\langle C_6^B\rangle}{12}\left[\frac{1}{(d/2+\xi-z)^3}+\frac{1}{(d/2+\xi+z)^3}-\frac{1}{(d/2-z)^3}-\frac{1}{(d/2+z)^3}\right]-\frac{\langle C_{12}^B\rangle}{90}\left[\frac{1}{(d/2+\xi-z)^9}+\frac{1}{(d/2+\xi+z)^9}-\frac{1}{(d/2-z)^9}-\frac{1}{(d/2+z)^9}\right]\right\} \quad (6)$$

$$V^3_{1B3}(d,\xi,z) = \frac{2\pi\Phi_1\mathcal{A}}{\xi}\left\{(d/2+\xi)\left[\frac{\langle C_6^B\rangle}{12}\left[\frac{1}{(d/2+\xi-z)^3}+\frac{1}{(d/2+\xi+z)^3}\right]-\frac{\langle C_{12}^B\rangle}{90}\left[\frac{1}{(d/2+\xi-z)^9}+\frac{1}{(d/2+\xi+z)^9}\right]\right]-\frac{d}{2}\left[\frac{\langle C_6^B\rangle}{12}\left[\frac{1}{(d/2-z)^3}+\frac{1}{(d/2+z)^3}\right]-\frac{\langle C_{12}^B\rangle}{90}\left[\frac{1}{(d/2-z)^9}+\frac{1}{(d/2+z)^9}\right]\right]+\frac{\langle C_6^B\rangle}{24}\left[\frac{1}{(d/2+\xi-z)^2}+\frac{1}{(d/2+\xi+z)^2}-\frac{1}{(d/2-z)^2}-\frac{1}{(d/2+z)^2}\right]-\frac{\langle C_{12}^B\rangle}{720}\left[\frac{1}{(d/2+\xi-z)^8}+\frac{1}{(d/2+\xi+z)^8}-\frac{1}{(d/2-z)^8}-\frac{1}{(d/2+z)^8}\right]\right\} \quad (7)$$

When $\xi \to 0$, we have a hard interface and $U_{1B3}(d,\xi,z)$ reduces to

$$U_{1B3}(d,0,z) = 2\pi\Phi_1\mathcal{A}\left\{\frac{-\langle C_6^B\rangle}{12}\left[\frac{1}{(d/2-z)^3}+\frac{1}{(d/2+z)^3}\right]+\frac{\langle C_{12}^B\rangle}{90}\left[\frac{1}{(d/2-z)^9}+\frac{1}{(d/2+z)^9}\right]\right\} \quad (8)$$

Here $\mathcal{A}$ is the area (in nm^2) of the faces of the crystals, Φ_1 is the number density of atomic moieties/nm^3 in the crystalline solids, and the total energy of the solid-oil interaction can be obtained by summing over all oil atomic moieties, B.

Oil density between the nanocrystals. We carried out simulations of the two systems, [1] $\xi = 0$ and [2] $\xi \neq 0$, with the requirement that the chemical potential of the system of Figure 1D and Figure 2 was equal to that of the bulk. The intent was to discover the response of a system that attempts to trap triolein oil between two parallel tristearin CNPs, the surfaces of which are "hard" or "soft" and to answer the question, is the oil binding capacity of a system with soft surfaces higher than that with hard surfaces. Finally we studied a system with $\xi = 0$ for which the oil density of the system of Figure 1D was constrained to be constant and equal to that of the bulk. The intent of this was to compare it with our simulation results of [1]. In order to evaluate the total energy, we need the number density in the nanocrystals. For a triolein or a tristearin molecule, the average mass per moiety is $\sim 2.35\times10^{-23}$ gm. Using a pycnometer, our measurements gave a density for FHCO of 1.03×10^{-21} gm/nm^3 at room temperature (~25C) which yielded a number density of $\Phi_1 \approx 44.0$ moieties/nm^3. Using a Mettler Toledo DE 40 density meter, we measured the density of HOSO to be 0.9016×10^{-21} gm/nm^3, and, from this, we calculated the number density in the bulk fluid phase to be $\Phi_2 \approx 38.5$ moieties/nm^3. Both density measurements were carried out at lab temperature (~25C).

Oil binding capacity. We define oil binding capacity, $B(W)$ as

$$B(W) = \frac{\rho(W)}{\rho_{bulk}} \qquad (9)$$

where ρ is the oil density in an environment, *W*, or in the bulk, and *W* describes the particular environment in which we are interested. In the case of the system of Figure 1D, the environment is defined by the distance, *d*, and the average number density, $<\Phi(d)>$, so that we would have,

$$B(d) = \frac{<\Phi(d)>}{<\Phi_{bulk}>} \qquad (10)$$

This definition, which compares the density of the oil trapped between nanoplatelets to the density of oil in the bulk, differs from that of Omonov et al. (equation 1)[41] who use the ratio of the mass of bound liquid oil to the solid fat content. Our computation of the amount of oil that can be "bound" between a pair of parallel surfaces is best quantified as we have done it. Our results should not be interpreted beyond what they say: that the density of oil in equilibrium between a pair of parallel CNP surfaces, much larger than the size of the oil molecules, can be changed depending upon the characteristics of the solid surfaces.

Results and Discussions

Here we describe and discuss the results of the two cases, [1] $\xi = 0$ and [2] $\xi \neq 0$. Before that, however, it is worthwhile making a comment about the molecular organization of the liquid oil phase. We have not analysed our data for, for example, the existence of density fluctuations or the appearance of short-range order. The question of whether short-range order such as discotics or semi-ordered hydrocarbon chain conformations (e.g., nematic structures) appear in a liquid TAG phase[42-45] was addressed by Pink *et al.*[46] who modelled the solid-liquid phase transition in symmetric saturated TAGs. They showed that transition enthalpy and Raman spectroscopy data did not support those proposals and that a $d \approx 4.6$Å line in X-ray or neutron scattering data appeared in a disordered liquid TAG phase and did not indicate a discotic phase.

[1] $\xi = 0$. ***Chemical potential of bulk and system of Figure 1D are equal***. We achieved this condition by adjusting the average oil number density, $< \Phi(d) >$, in the system so as to make the chemical potentials equal.. The dependence of the number density as a function of z for a given CNP separation, d, is shown in Figure 3.

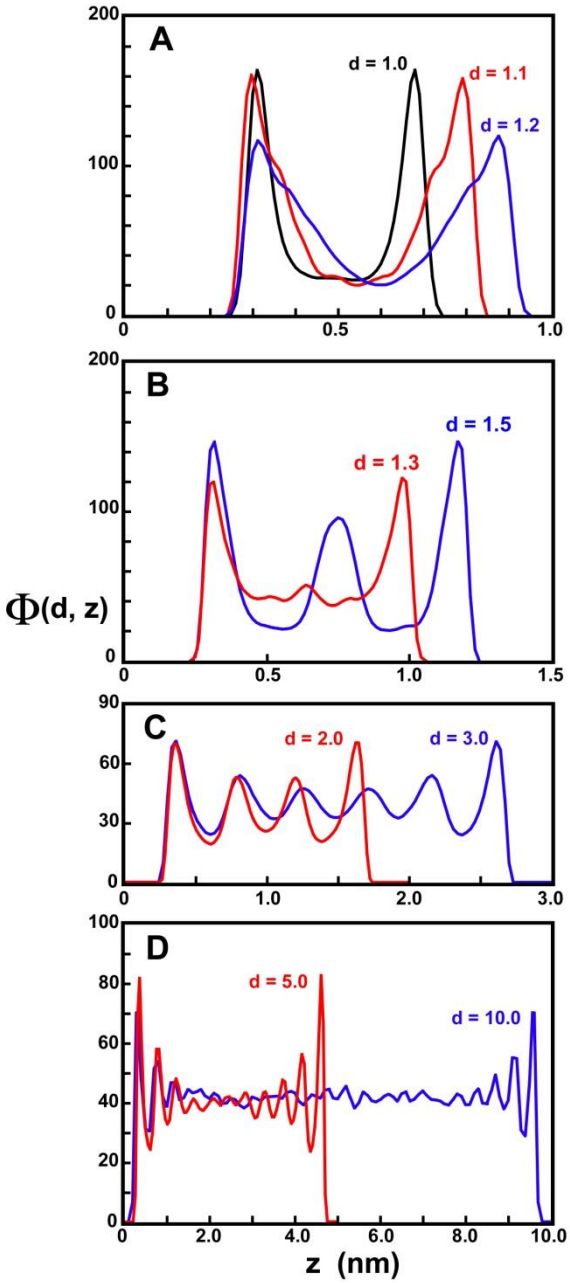

Figure 3. Triolein between two parallel-face tristearin CNPs. Number density distribution of centres of atomic moieties, $\Phi(d,z)$, as functions of the separation distance d. That there are regions near the faces where the number density of centres is zero does not mean that there is zero atomic electron density located there. **A:** d= 1.0 (black), 1.1 (red), 1.2 (blue) nm. **B:** d = 1.3 (red), 1.5 (blue) nm. **C:** d= 2.0 (red), 3.0 (blue) nm. **D:** d = 5.0 (red), 10.0 (blue) nm. Note that the vertical and horizontal scales differ from A to D.

Figure 3 shows the existence of equilibrium oscillations in the number densities, $\Phi(d,z)$, of centres of triolein atomic moieties calculated by counting their number in slices 0.1 nm thick filling space between the solid faces. We ignored consideration of whether fractions of atomic moieties extended over different slices. The density is highest near the faces because the attractive interaction of solid tristearins with the oil is greater than are the oil-oil interactions. The areas under the curves will yield the average number density, $<\Phi(d)>$, of the triolein as a function of d (Figure 4). Such number density oscillations are typical of systems such as these as reported elsewhere (above).

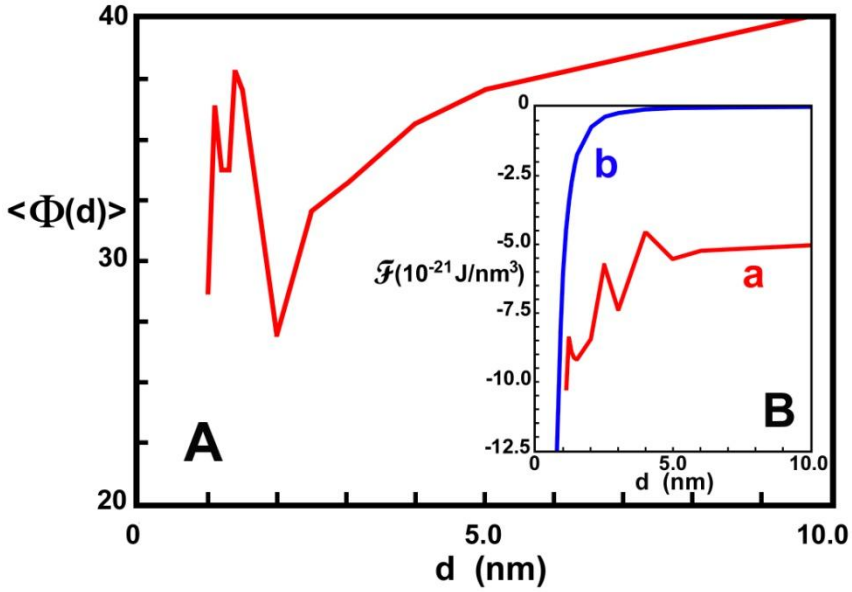

Figure 4. Triolein between two parallel-face tristearin CNPs. **A:** Average triolein number density, $<\Phi(d)>$, as a function of CNP separation distance, d. **B:** Helmholtz free energy density, F, (10^{-21} J/nm^3) (a). For comparison the energy density of the continuum 6-12 potential model is shown (b).

Figure 4 shows that the average triolein number density, $<\Phi(d)>$, decreases as the CNPs become closer together, until it achieves a local minimum at $d \approx 2$ nm. As d decreases further, the average density increases. As $d \to 0$, $<\Phi(d)>$ decreases towards zero. Since $<\Phi_{bulk}>$ is a constant, it is clear that the oil binding capacity, equation (10), changes like $<\Phi(d)>$. Moreover, in order to maximize the amount of bound oil in the system, we must identify local maxima in $<\Phi(d)>$ that coincide with local minima in the free energy density, such as occurs around $d \approx 1.5$ nm. As an insert we see energy densities as functions of

d in units of 10^{-21} J/nm^3. The free energy density of the model of Figure 1D when the chemical potentials of the bulk and the system of oil between nanocrystals are equal, exhibits local minima at $d \approx 3$ nm and, more markedly but shallower, at $\sim 1.4-2$ nm (curve a). Even ignoring the peaks in the free energy, its dependence upon CNP separation distance is not $1/d^2$ as it would be if we modelled this system as a continuum Lennard-Jones fluid. The reason for this is that the average oil number density is decreasing as $d \to 0$. We compared this result with the energy density of the continuum 6-12 potential model of the nanocrystals with no oil between them (curve b). In both cases (a) and (b), the global free energy density minimum occurs when $d \approx 0.275$ nm, for which there is no oil between the CNPs. The difference between curves (a) and (b) as $d \to \infty$ is the binding energy of the oil to the surfaces of the CNPs.

The result of Figure 4A is in accord with what is known about polymers in confined spaces, e.g, between colloidal particles, and depletion forces[47-52].

[2] $\xi \neq 0$. ***Chemical potential of bulk and system of Figure 1D are equal***. As in [1], we achieved this condition by adjusting the average oil number density, $<\Phi(d)>$, in the system so as to make the chemical potentials equal. We chose $\xi = 4$ nm. The dependence of the number density as a function of z for a given CNP separation, d, is shown in Figure 5 where we compare it to some of the results of Figure 3.

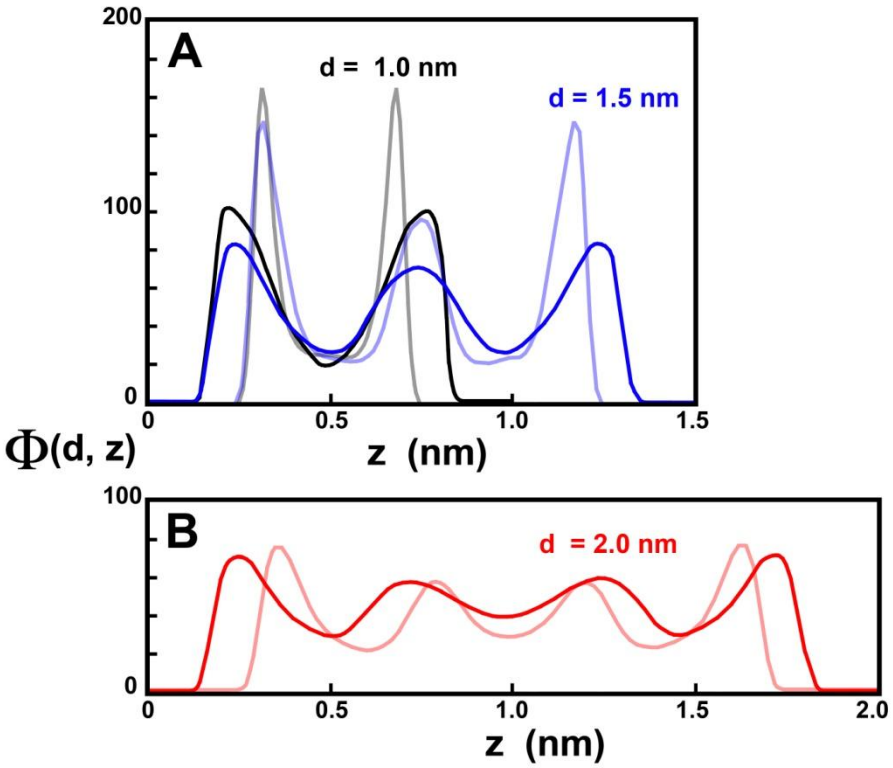

Figure 5. Triolein between two parallel-face tristearin CNPs each of which possesses a soft interface of thickness $\xi = 4$ nm. Number density distribution of centres of atomic moieties, $\Phi(d, z)$, as functions of the separation distance d. See Figure 2 for the definition of separation distance when $\xi \neq 0$. Bright colours are $\xi \neq 0$ and pale colours are $\xi = 0$ for comparison. **A:** *d*= 1.0 nm (black), 1.5 nm (blue). **B:** *d*= 2.0 (red) nm.

We see that the effect of the soft surfaces are to cause the oscillations to be spread out compared to the case of the hard surfaces. The areas under the curves multiplied by the areas of the surfaces will give the average number density. Even from these three values of d we expect that the average number density for the soft surface cases for $d = 1.0$ and $d = 2.0$ nm will be larger than those for the respective hard surface cases. This is confirmed in Figure 6 where we see that the average number density for the system with soft surfaces is essentially constant as d changes.

That the density oscillations extend into the region of low-density soft surface (Figure 2) is an indication that the triolein molecules can occupy such spaces and is likely the reason that the average density remains approximately constant as d decreases.

Using our definition of oil binding capacity (equation (8)) and in the absence of measurements of the oil binding capacity of tristearin CNPs in triolein oil,, we predict that, while tristearin CNPs with hard surfaces will exhibit low oil binding capacity, the same CNPs coated with layers of soft material could have high oil binding capacity.

We found no ordering of the triolein molecules at either of the CNP surfaces which shows the fundamental difference between hydrophilic mica and hydrophobic tristearin surfaces. No anhydrous triolein ordering was observed [33,34] for mica surfaces rendered hydrophobic via phospholipid self-assembly on the surface, and our simulations are in accord with that result.

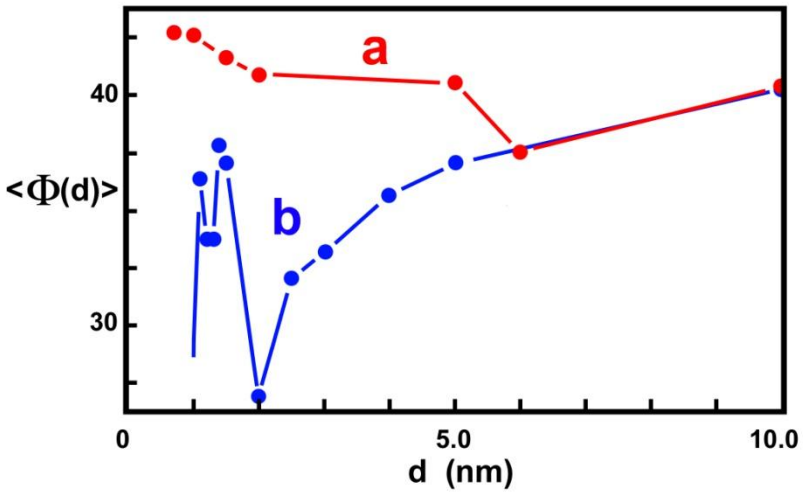

Figure 6 Triolein between two parallel-face tristearin CNPs. Average triolein number density, $<\Phi(d)>$, as a function of separation distance, d. Average number density for the case of soft surfaces (a, red) and hard surfaces (b, blue).

Conclusions

(i) We found, as expected, that number density oscillations between parallel-faced tristearin particles possessing hard surfaces arose in the oil and that the average oil number density exhibited a non-monotonic decrease of up to ~40% when d became <10 nm. An analogous effect has also been seen in simulations of van der Waals spheres and hard spheres in nanotubes[51,52]. This result shows that, when two fat particles with hard surfaces are separated by a few nanometers, the oil between them can be expelled into the surrounding oil. We defined oil binding capacity, $B(d)$, and predict that this result implies that $B(d)$ of tristearin particles with hard surfaces in triolein oil is low. Although the free energy exhibits a global minimum when $d \approx 0.275$ nm, there is then no oil between the hard-surface CNPs. With oil between them, local minima in the free energy density appeared at $d \approx 3$ nm and $d \approx 1.5-2.0$ nm. A similar system in which the average oil density between the CNPs was constrained to be constant also exhibited number density oscillations. We have not reported these results here. Our results invalidate the belief that the van der Waals energy of interaction between the two CNPs of Figure 1 exhibits a $1/d^2$ dependence with a constant Hamaker

coefficient. We carried out analytical and numerical studies and found that the energy density involves, not only the $1/d^3$ term from equation (2), but also terms in $1/d$ and $1/d^2$. One can define a d-dependent Hamaker coefficient, $A_H(d)$, if one specifies that the attractive energy is $-A_H(d)/12\pi d^2$, but this rather defeats the purpose of this quantity.

(ii) We modelled tristearin CNPs which possessed soft surfaces in order to see whether such a system would have a higher oil binding capacity (equation (10)). We found that, although number density oscillations also appear, as we would expect, their maxima and minima are more spaced out (the characteristic wavelengths are longer) than in the case of hard surfaces. More importantly, the average triolein density between the CNPs exhibits an essentially constant value for all values of d. This means that the oil binding capacity of such fats can be high.

We believe that our results are the first to address the problem of identifying what factors contribute towards the oil binding capacity of triglyceride oils by triglyceride solids on the nanoscale. Our conclusions concerning this is that a lower oil binding capacity is brought about by the packing of triolein molecules at the tristearin surface, resulting in it being entropically favourable for the oil between the CNPs to be depleted and to move to the bulk. In order to overcome this, it is advantageous that the CNP surface be coated with those minority component oils which could present an effective soft surface.

Acknowledgements

We thank Dr. Nuria Acevedo and Ms. Bonnie Quinn for information and discussions. We also thank two referees for some excellent and thoughtful comments. DAP and AGM thank NSERC of Canada, AFMNet and ACEnet for support. CJM thanks NSERC for a USRA. CBH was supported by U.S. NSF Grant No. DMR-0906618.

References

1. A. K. Sum, M. J. Biddy, J. J. dePablo and M. J. Tupy, *J. Phys. Chem. B,* 2003, **107**, 14443-14451.
2. A. Hall, J. Repakova and I. Vattulainen, *J. Phys. Chem. B*, 2008, **112**, 13772-13782.
3. W. D. Hsu and A. Violi, *J. Phys. Chem. B,* 2009, **113**, 887-893.
4. N. T. Bendsen, R. Christensen, E. M. Bartels, and A Astrup, *Eur. J. Clin. Nutr.*, 2011, **65**, 773–83.

5. S. K. Gebauer, J.-M. Chardigny, M. U. Jakobsen, B. Lamarche, A. L. Lock, S. D. Proctor, and D. J. Baer, *Adv. Nutr.*, 2011, **2**, 332–354.
6. E. Decker, *ePerspective*.2013. http://foodtecheperspective.wordpress.com/2013/11/13/the-impact-and-consequences-of-banning-trans-fatty-acids/
7. N. C. Acevedo and A. G. Marangoni, *Cryst. Growth Des.*, 2010, **10**, 3327–3333.
8. N. C. Acevedo, in *Structure-Function Analysis of Edible Fats*, ed. A. G. Marangoni, AOCS Press, Urbana, IL, 2012, pp. 5–24.
9. N. C. Acevedo, F. Peyronel, and A. G. Marangoni, *Curr. Opin. Colloid Interface Sci.*, 2011, **16**, 374–383.
10. F. Peyronel, J. Ilavsky, G. Mazzanti, A. G. Marangoni, and D. A. Pink, *J. Appl. Phys.*, 2013, In Press.
11. C. J. MacDougall, M. Shajahan Razul, E. Papp-Szabo, F. Peyronel, C. B. Hanna, A. G. Marangoni, and D. A. Pink, *Faraday Disc.*, 2012, **158**, 425–433.

12. R. G. Horn and J. N. Israelachvili, *Macromolecules*, 1988, **21**, 2836–2841.
13. W. D. Kaplan and Y. Kauffmann, *Annu. Rev. Mater. Res.*, 2006, **36**, 1–48.
14. F. Porcheron, M. Schoen, and A. H. Fuchs, *J. Chem. Phys.*, 2002, **116**, 5816–5824.
15. J.-C. Wang and S. Saroja, *Mol. Simul.*, 2003, **29**, 495–508.
16. R. Evans, *J. Phys. Condens. Matter*, 1990, **2**, 8989–9007.
17. R. Batman and P. D. Gujrati, *J. Chem. Phys.*, 2007, **127**, 084904.
18. J. N. Israelachvili, *Surf. Sci. Rep.*, 1992, **14**, 109–159.
19. X.-Y. Liu, P. Bennema, L. A. Meijer, and M. S. Couto, *Chem. Phys. Lett.*, 1994, **220**, 53–58.
20. A. Yethiraj and C. K. Hall, *J. Chem. Phys.*, 1989, **91**, 4827–4837.
21. A. Yethiraj and C. K. Hall, *Macromolecules*, 1990, **23**, 1865–1872.
22. R. von Klitzing, E. Thormann, T. Nylander, D. Langevin, and C. Stubenrauch, *Adv. Colloid Interface Sci.*, 2010, **155**, 19–31.
23. Y. Termonia, *Polymer*, 2011, **52**, 5193–5196.
24. H. K. Christenson, D. W. R. Gruen, R. G. Horn and J. N.Israelachvili, *J. Chem. Phys.*, 1987, **87**, 1834–1841.
25. P. Smith, R. M. Lynden-Bell and W. Smith, *Mol. Phys.*, 2000, **98**, 255–260.
26. F. Porcheron, B. Rousseau and A. H. Fuchs, *Mol. Phys.*, 2002, **100**, 2109–2119.
27. C. J. Mundy, S. Balasubramanian, K. Bagchi, J. I. Siepmann and M. L. Klein, *Faraday Discuss.*, 1996, **104**, 17–36.
28. N. Maeda and H. K. Christenson, *Colloids Surfaces A Physicochem. Eng. Asp.*, 1999, **159**, 135–148.

29. V. A. Parsegian, *Van der Waals Forces. Handbook for Scientists and Engineers*, Cambridge University Press, 2005.
30. J. N. Israelachvili, Intermolecular and Surface Forces, Academic Press, London, 3rd Edition, 2011.
31. P. M. Claesson, A. Dedinaite, B. Bergenståhl, B. Campbell and H. Christenson|, *Langmuir* 1997, **13**, 1682-1688
32. A. Dedinaite, P. M. Claessen, B. Bergenstahl and B. Campbell, *Food Hydrocolloids*, 1997, **11**, 7-12,
33. A. Dedinaite, P. M. Claesson, B. Campbell and H. Mays, *Langmuir* 1998, **14**, 5546-5554
34. A. Dedinaite and B. Campbell, *Langmuir* 2000, **16,** 2248-2253
35. H. C. Hamaker, *Physica*, 1937, **4**, 1058–1072.
36. O. Berger, O. Edholm, and F. Jähnig, *Biophys. J.*, 1997, **72**, 2002–13.
37. B. Hess, C. Kutzner, D. van der Spoel, and E. Lindahl, *J. Chem. Theory Comput*, 2008, **4**, 435–447. See also www.gromacs.org, GROMACS user manual version 4.0, gromacs4_manual.pdf
38. H. J. C. Berendsen, D. van der Spoel, and R. van Drunen, *Comput. Phys. Commun*, 1995, **91**, 43–56.
39. C. Kutzner, D. van der Spoel, M. Fechner, E. Lindahl, U. W. Schmitt, B. L. de Groot, and H. Grubmüller, *J. Comput. Chem.*, 2007, **28**, 2075–2084.
40. C. B. Hanna, D. A. Pink, and B. E. Quinn, *J.Phys Condens.*, 2006, **18**, 8129–8137.
41. T. S. Omonov, L. Bouzidi and S. S. Narine, *Chem. Phys. Lipids*, 2010, **163**, 728–740

42. K. Larsson, *Fette, Seifen, Anstrichm*., 1972, **74**, 136.
43. K. Larsson, *J. Am. Oil Chem. Soc.* 1992, **69**, 835-836.
44. D. J. Cebula, D. J. McClements, M. J. W. Povey, and P. R. Smith, *J. Am. Oil Chem. Soc.*, 1992, **69**, 130-136.
45. R. Corkery, P. R. Smith, D. A. Pink, C. B. Hanna, and D. Rousseau, *Langmuir*, 2007, **23**, 7241-7246.
46. D. A. Pink, C. B. Hanna, C. Sandt, A. J. MacDonald, R. MacEachern, R. Corkery and D. Rousseau, *J. Chem. Phys*., 2010, **132**, 54502-54513.

47. S. Asakura and J. Oosawa, *J. Polym Sci*, 1958, **32**, 183.
48. P. Jenkins and M. Snowden, *Adv. Colloid Interface Sci.*, 1996, **68**, 57–96.
49. A. Meller and J. Stavans, *Langmuir*, 1996, **12**, 301–304.
50. R. Tuinier, J. Rieger, and C. G. de Kruif, *Adv. Colloid Interface Sci.*, 2003, **103**, 1–31.
51. S. Egorov, *Phys. Rev. E*, 2004, **70**, 031402.
52. A. I. Chervanyov, *Phys. Rev. E*, 2011, **83**, 061801.

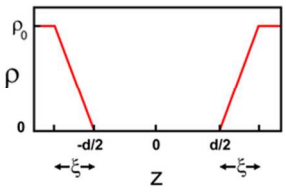

Figure 2. Mass density cross section through crystalline nanoplatelets showing soft interfaces of thickness ξ

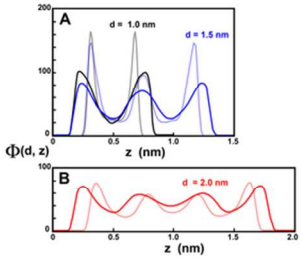

Figure 5. Triolein number density oscillations as functions of distance, z, between the surfaces when they are separated by a distance d. Coated surfaces bold, uncoated surfaces light.

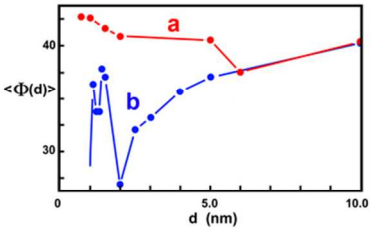

Figure 6. Average triolein number density as a function of distance, d, between the tristearin nanoplatelets.
a: coated surfaces
b: uncoated surfaces.

39x19mm (600 x 600 DPI)